Journal of the Korean Society of Propulsion Engineers
Vol. 19, No. 5, pp. 31-36, 2015

Research Paper
DOI: http://dx.doi.org/10.6108/KSPE.2015.19.5.031

이중 모드 스크램제트 격리부 특성에 대한 수치해석적 연구

Ruoyu Deng[a] · 김희동[a,*] · Yingzi Jin[b]

Numerical Study on the Characteristics of Dual-Mode Scramjet Isolator

Ruoyu Deng[a] · Heuy Dong Kim[a,*] · Yingzi Jin[b]
[a] *Department of Mechanical Engineering, Andong National University, Korea*
[b] *College of Mechanical Engineering & Automation, Zhejiang Sci-Tech University, China*
[*] *Corresponding author. E-mail: kimhd@anu.ac.kr*

ABSTRACT

As one of the most promising propulsive systems in the future, the dual-mode scramjet engine has drawn the attention of many researches. Detailed flow features concerned with the isolator play an important role in the dual-mode scramjet system. The 2D numerical method has been used for the dual-mode scramjet with wind tunnel. To validate the ability of the numerical model, numerical results have been compared with the experimental results. Overall pressure distributions show quite good match with the experimental results. Back pressure has been studied for maximum pressure rising. According to the results, pressure distribution of supersonic inlet section is not influenced by back pressure. The shock train is pushed towards upstream as the back pressure increases. The maximum value of back pressure without inlet unstart goes up rapidly and then keeps constant when the isolator length increases. The optimal length of isolator section (L/H_{th}) is 8.7 in this model.

초록

이중 모드 스크램제트 엔진은 미래 가장 촉망받는 시스템 중 하나로, 많은 연구자들에게 각광받고 있다. 이중 모드 스크램제트 엔진 시스템에서 격리부와 관련된 유동 특징들은 중요한 역할을 한다. 본 연구에서 풍동을 가진 이중 모드 스크램제트 엔진을 조사하기 위해 2차원 수치해석을 수행하였다. 계산방법의 타당성을 검증하기 위하여 실험결과와 비교하였으며, 수치해석 결과는 실험값과 비교하여 전체적으로 압력 분포가 잘 일치하였다. 배압은 최대 압력 상승을 분석하기 위해 연구되었다. 그 결과 초음속 흡입구 영역의 압력 분포는 배압에 영향을 받지 않았으며, 배압이 증가함에 따라 Shock train은 상류 쪽으로 밀려나갔다. 격리부의 길이가 증가함에 따라 최대 배압값은 입구 불시동 없이 급격히 증가한 후 일정하게 유지되었으며, 격리부 영역의 최적 길이(L/H_{th})는 8.7이다.

Key Words: Dual-mode Scramjet(이중 모드 스크램제트), Isolator(격리부), Supersonic Inlet(초음속 흡입구), Back Pressure(배압)

Received 2 June 2015 / Revised 19 August 2015 / Accepted 24 August 2015

pISSN 1226-6027 / eISSN 2288-4548
[이 논문은 한국추진공학회 2015년도 춘계학술대회(2015. 5. 28-29, 부산 해운대 그랜드호텔) 발표논문을 심사하여 수정 · 보완한 것임.]

Nomenclature

H_{th} : isolator height

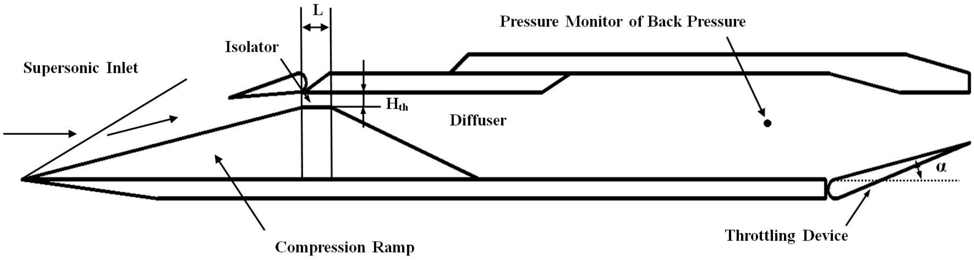

Fig. 1 Schematic diagram of inlet isolator in dual-mode scramjet.

L	: isolator length
P_1	: static pressure in the free stream
P_b	: back pressure
P_{max}	: maximum back pressure in a isolator length
X	: x-coordinate

1. Introduction

In a dual-mode scramjet, combustion can either occur at subsonic or supersonic speeds, or a mixture of the two. As the Mach number is increased past about 4, the subsonic ramjet transitions into the dual-mode regime, where the inlet Mach number is increased enough and a pre-combustion shock train is generated. The isolator is designed to prevent this shock train from reaching the inlet to prevent catastrophic inlet unstart. The numerical simulation will be performed at speed of Mach 4 because significant effects on mode transition occur at this speed. As the Mach number is further increased past about 6, the pre-combustion shock train moves out of the isolator and the combustor operates in the supersonic mode.

The properties of inlet isolator are critical in improving the performance of dual-mode scramjet. The pressure distributions and lengths of pre-combustion shock trains have been studied by some researchers[1]. Numerical and experimental methods were performed to investigate the use of swept-ramp configurations for improving the performance of a rectangular scramjet isolator [2,3]. Experimental studies were conducted in the cold flow Mach 4 Blowdown Facility at the Langley Research Center to investigate inlet-isolator performance in the scramjet engine[4]. Effects of temperature and heat transfer on shock train structures and isolator performance were investigated both experimentally and numerically[5]. Numerical approaches were utilized to better determine the shock train leading edge location of a typical Mach 2 nozzle-isolator configuration [6,7]. Although many researches on developing the dual-mode scramjet isolator were done during past years, there were still many difficult problems in the isolator application.

The purpose of the present study has been to explore these issues for dual-mode scramjet isolator. Before studying the isolator performance, a validation description of the numerical model has been bring into effect. Numerical model has been established to investigate the details of shock system in the isolator. Different parameters that affect isolator performance, such as isolator length and back pressure, have studied in numerical model.

2. Model description

2.1 Base model

The two dimensional inlet isolator model has been established to replicate the generic features of the supersonic air breathing propulsion system. It included supersonic inlet compression, isolator and the diffuser downstream of the isolator. The schematic diagram of inlet isolator in dual-mode scramjet is shown as Fig. 1.

The wetted surfaces that enclose the flow path consist of three major flow categories: inlet, isolator and combustion diffuser. The 11 degree compression ramp is 248 mm long. The cowl length is 63.5 mm and inlet convergence angle is 8.8 degree. The throat height (H_{th}) is 10 mm for all conditions. The 20 degree expansion nozzle is used in the diffuser. The 2D throttling device has been used to change back pressure. The back pressure has been monitored in the diffuser chamber, as shown in the Fig. 1. The length of movable flap in throttling device is 150mm.

2.2 Numerical modeling

For the CFD simulation software, ANSYS Fluent 14.0 is chosen to calculate the flow structure of the dual-mode scramjet isolator. The working fluid is considered as ideal gas in this study. The model of dual-mode scramjet has been installed in the wind tunnel. For the numerical model, the inlet and outlet boundary condition have been set up on the wind tunnel. Two-equation standard k-ε turbulence model has been used. The 2D structured mesh is used for all regions. Mesh independent study is conducted with different grid distribution in order to select the better grid. The mesh of all domains are composed of 0.4 million mapped hexagonal elements. Pressure far field condition has been set at stream inlet and side of the wind tunnel. Pressure outlet condition has been used in downstream outlet. The free-stream boundary condition has been used in the supersonic tunnel of Mach 4. The static pressure and Reynolds number in the tunnel are 8729 Pa and $16\text{x}10^6$, respectively. The total temperature in tunnel flow is 300 K in this study.

3. Results and discussion

3.1 Validation

To validate the numerical model, the experimental data of Saied et al.[3] is used for comparison. In order to investigate the flow field, pressure distribution in numerical model is compared with the experimental result. Numerical and experimental static wall pressure distributions for $L/H_{th}=2.7$ and $P_b/P_1=12.83$ are shown in Fig. 2. The pressure distributions are normalized by the static pressure P_1 of the free stream tunnel. Fig. 3 shows Mach number contour of inlet isolator in free stream condition. The first pressure rise is caused by the inlet contraction. The expansion wave occurs at the end of inlet and isolator. So the pressure goes down in these two positions. There are shock reflection and boundary layer separation in the diffuser part downstream of isolator. The pressure variation can be observed clearly due to the complex shock system.

3.2 Isolator performance with isolator lengths

The movable flap on the throttling device has been closed until the throttling device forced a shock train upstream toward the inlet throat. Back pressuring of the isolator and inlet has been continued by closing the

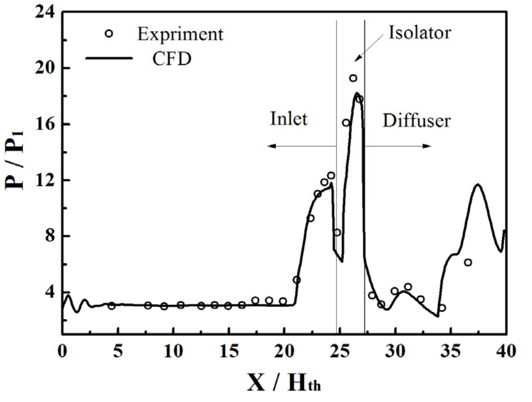

Fig. 2 Numerical and experimental pressure profiles (L/Hth=2.7 and Pb/P1=12.83).

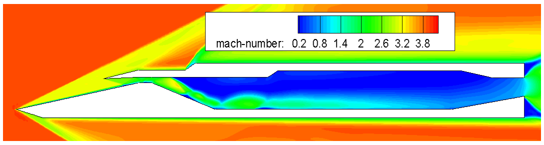

Fig. 3 Mach contour of inlet isolator (L/H_{th}=2.7 and P_b/P_1=12.83).

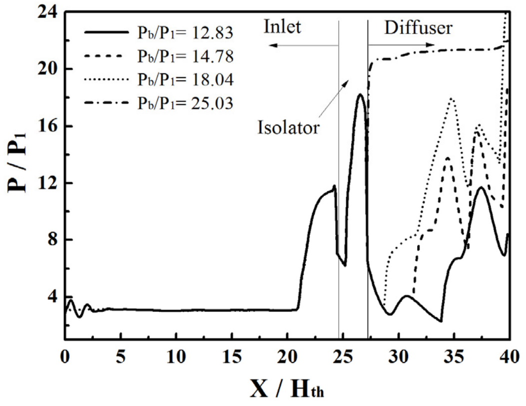

Fig. 4 Body wall pressure profiles with different back pressures (L/H_{th}=2.7).

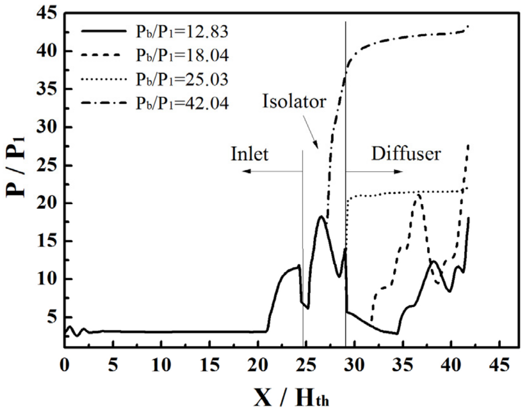

Fig. 5 Pressure profiles with different back pressures (L/H_{th}=4.7).

throttling device flap until the inlet unstart. The minimum and maximum throttling back pressures simulate the effects of no-fuel and maximum-fuel fraction that can be added without unstarting the inlet.

For optimum isolator effect, different back pressures should be researched. The body wall pressure profiles with different back pressures for L/H_{th}=2.7 are shown in Fig. 4. It is indicated that pressure profiles of inlet section are exactly the same in different back pressures. The upstream condition of isolator should not be affected by the back pressure variation before unstarting the inlet. In this figure, the diffuser pressure increase gradually as the back pressure increases. There are two situations that happens at the end of the isolator, supersonic and subsonic. For the supersonic case, the supersonic flow is accelerated at the beginning of the diffuser, and then the boundary layer separation occurs in the second part of diffuser. For the subsonic case, the pressure goes up at the end of isolator due to the divergent diffuser.

The constant-area variable-length isolator followed by a diffuser section has been researched. The inlet section is fixed in all configurations. The pressure profiles in different isolator lengths are shown in Fig. 5 and Fig. 6, respectively. The shock train is pushed toward the isolator entrance as back pressure increases until it reaches the maximum value. The shock strain will be initiated inside the facility nozzle

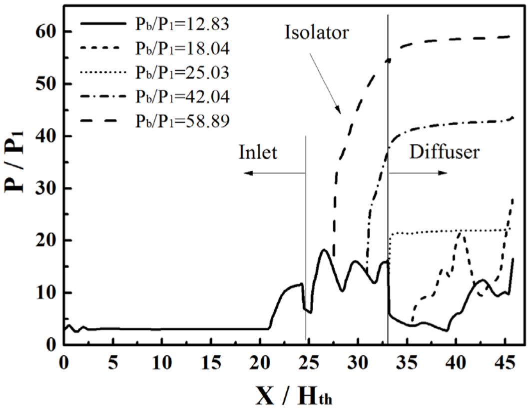

Fig. 6 Pressure profiles with different back pressures (L/H_{th}=8.7).

if the back pressure exceeds the maximum value, which could cause undesired engine unstart under actual flight conditions. Fig. 7 shows the density gradient of isolator in different back pressures for the case of L/H_{th}=8.7. It can be observed clearly that there are oblique shock reflection and expansion wave in the isolator section. The shock train is pushed towards upstream as the back pressure increases. The increasing process of back pressure should be stopped before the shock train reaches the isolator entrance.

The isolator length is shorter than the shock train length when the back pressure is quite small. Different isolator lengths have been studied for the optimal value. Maximum back pressure with isolator lengths are shown in Fig. 8 The isolator lengths are normalized by the isolator height H_{th}. It can be observed, when the isolator length increases, the maximum back pressure P_{max} without inlet unstart goes up rapidly and then the rising process slows down. The optimal isolator length (L/H_{th}) is 8.7 in this model. The maximum back pressure will decrease gradually due to the additional viscous loss if the isolator length increases further.

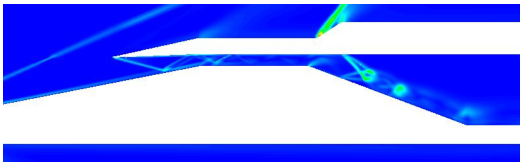

a)P_b/P_1=18.04

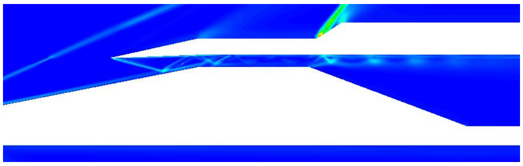

b) P_b/P_1=25.03

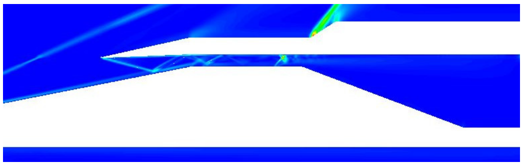

c) P_b/P_1=42.04

d) P_b/P_1=58.89

Fig. 7 Density gradient of inlet isolator with different back pressures (L/H_{th}=8.7).

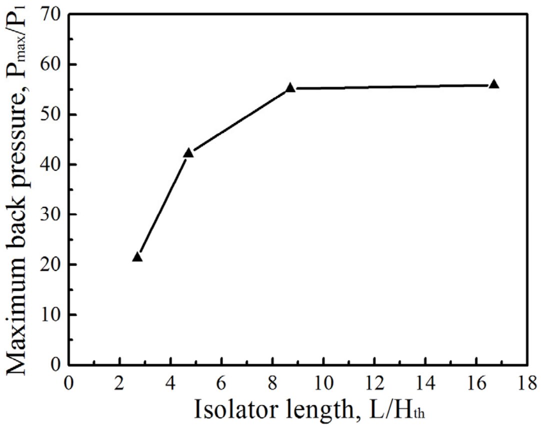

Fig. 8 Maximum back pressure with different isolator lengths.

4. Conclusions

Numerical approach has been taken in order to investigate the inlet isolator of dual-mode scramjet. Fluent 14.0 has been used in order to simulate the flow field inside the isolator. Different factors have been investigated in this paper, such as back pressure and isolator length. In order to validate the numerical model, numerical results are compared with the experimental results. Overall pressure distributions show quite good match. There are two situations that happens at the end of the isolator, supersonic and subsonic. The pressure distribution in the diffuser is decided by this situations. Pressure profiles of inlet section are exactly the same in different back pressures, and the shock train is pushed toward upstream as the back pressure increases. The maximum back pressure without inlet unstart goes up rapidly and keep constant when the isolator length increases in this study. The optimal isolator length (L/H_{th}) is 8.7 in this model. Further works is going on to research the unsteady process with back pressure variation.

Acknowledgment

This work was supported by Advanced Research Center Program (NRF-2013R1A5A1073861) through the National Research Foundation of Korea (NRF) grant funded by the Korea government (MSIP) contracted through Advanced Space Propulsion Research Center at Seoul National University. (Project Number: 0659-20140012)

References

1. Matsuo, K., Miyazato, Y. and Kim, H.D., "Shock Train and Pseudo-shock Phenomena in Internal Gas Flows," *Progress in Aerospace Sciences*, Vol. 35, No. 1, pp. 33-100, 1999.
2. Lin, K.C., Tam, C.J., Jackson, K., Kennedy, P. and Behdadnia, R., "Experimental Investigations on Simple Variable Geometry for Improving Scramjet Isolator Performance," *43rd AIAA/ASME/SAE/ASEE Joint Propulsion Conference & Exhibit*, Cincinnati, O.H., USA, AIAA 2007-5378, 2007.
3. Tam, C.J., Lin, K.C., Davis, D.L. and Behdadnia, R., "Numerical Investigations on Simple Variable Geometry for Improving Scramjet Isolator Performance," *42nd AIAA/ASME/SAE/ASEE Joint Propulsion Conference & Exhibit*, Sacramento, C.A., USA, AIAA 2006-4509, 2006.
4. Emami, S., Trexler, C.A., Auslender, A.H. and Weidner, J.P., "Experimental Investigation of Inlet-combustor Isolators for a Dual-mode Scramjet at a Mach Number of 4," *NASA TP* 3502, 1995.
5. Lin, K.C., Tam, C.J., Eklund, D.R., Jackson, K.R. and Jackson, T.A., "Effects of Temperature and Heat Transfer on Shock Train Structures inside Constant-area Isolators," *44th AIAA Aerospace Sciences Meeting and Exhibit*, Reno, N.V., USA, AIAA 2006-817, Jan. 2006.
6. Allen, J.B., Hauser, T. and Tam, C.J., "Numerical Simulations of a Scramjet Isolator using RANS and LES Approaches," *45th AIAA Aerospace Sciences Meeting and Exhibit*, Reno, N.V., USA, AIAA 2007-115, Jan. 2007.
7. Tam, C.J., Eklund, D. and Behdadnia, R., "Influence of Downstream Boundary Conditions on Scramjet-isolator Simulations," *26th AIAA Applied Aerodynamics Conference*, Honolulu, H.I., USA, AIAA 2008-6929, Aug. 2008.